Molecular Therapy
Nucleic Acids
Original Article

Evaluation of DNA minicircles for delivery of adenine and cytosine base editors using activatable gene on "GO" reporter imaging systems

Melissa M. Evans,[1,2,4] Shirley Liu,[1,2,4] Joshua S. Krautner,[1,2] Caroline G. Seguin,[1] Rajan Leung,[1,2] and John A. Ronald[1,2,3]

[1]Robarts Research Institute, University of Western Ontario, London, ON N6A 3K7, Canada; [2]Department of Medical Biophysics, University of Western Ontario, London, ON N6A 5C1, Canada; [3]Lawson Health Research Institute, London, ON N6C 2R5, Canada

Over 30,000 point mutations are associated with debilitating diseases, including many cancer types, underscoring a critical need for targeted genomic solutions. CRISPR base editors, like adenine base editors (ABEs) and cytosine base editors (CBEs), enable precise modifications by converting adenine to guanine and cytosine to thymine, respectively. Challenges in efficiency and safety concerns regarding viral vectors used in delivery limit the scope of base editing. This study introduces non-viral minicircles, bacterial-backbone-free plasmids, as a delivery vehicle for ABEs and CBEs. The research uses cells engineered with the "Gene On" (GO) reporter gene systems for tracking minicircle-delivered ABEs, CBEs, or Cas9 nickase (control), using green fluorescent protein (GFP^{GO}), bioluminescence reporter firefly luciferase (LUC^{GO}), or a highly sensitive Akaluciferase ($Akaluc^{GO}$) designed in this study. The results show that transfection of minicircles expressing CBE or ABE resulted in significantly higher GFP expression and luminescence signals over controls, with minicircles demonstrating the most substantial editing. This study presents minicircles as a new strategy for base editor delivery and develops an enhanced bioluminescence imaging reporter system for tracking ABE activity. Future studies aim to evaluate the use of minicircles in preclinical cancer models, facilitating potential clinical applications.

INTRODUCTION

Point mutations, involving single base pair alterations in DNA, underlie a wide spectrum of genetic diseases, including conditions such as sickle cell disease, Duchenne muscular dystrophy, β-thalassemia, and diverse types of cancer.[1–3] This class of mutations accounts for a significant portion, approximately 58%, of human pathogenic variants associated with disease.[4,5] The quest for technologies capable of accurately editing the genome, particularly concerning point mutations, has been a long-standing endeavor. Such capabilities hold the potential of providing solutions for genetic disorders arising from these mutations. Moreover, these innovative tools can be harnessed to induce point mutations aimed at deactivating target genes, including oncogenes in the context of cancer.

The advent of the clustered regularly interspaced short palindromic repeat (CRISPR) system in 2012 marked a revolutionary milestone in genome editing due to its simplicity, ease of design, and cost-effectiveness.[6,7] By generating double-stranded breaks (DSBs) in DNA, CRISPR facilitates targeted modification of specific sequences using a donor template. However, it is essential to recognize that CRISPR-mediated DSBs can cause unintended insertions or deletions, chromosome rearrangements, off-target effects, epigenetic modifications, DNA damage responses, and potential disruptions in gene regulation within functional genomic domains.[8]

To address some of the safety concerns associated with DSBs, Dr. David Liu and colleagues developed a novel CRISPR-based genome editing technology in 2016, called base editing.[9] This breakthrough method enables conversion of single nucleotide bases without creating DSBs, offering a safer alternative for precise genome editing. Base editors (BEs) consist of three key components: (1) a single guide RNA (sgRNA) for programmable targeting of a genomic locus, (2) a nucleobase deaminase responsible for catalyzing the base conversion, and (3) a partially enzymatically disabled Cas9 nickase (Cas9n), which induces a single-stranded nick, instead of a DSB, to promote mismatch repair.[9] Cytosine BEs (CBEs) induce cytosine-to-thymidine (C-to-T) conversions, while adenine BEs (ABEs) induce adenine-to-guanine (A-to-G) conversions.[9,10] Since their development, BEs have been successfully applied to correct point mutations linked to an array of diseases, including sickle cell disease,[11] Duchenne muscular dystrophy,[12,13] tyrosinemia,[14,15] inherited hearing loss,[16,17] and blindness[18,19] as well as cancer.[9,20]

While base editing has shown great promise in terms of versatility and safety, a significant challenge that remains is the efficient and safe

Received 11 December 2023; accepted 7 June 2024;
https://doi.org/10.1016/j.omtn.2024.102248.

[4]These authors contributed equally

Correspondence: John A. Ronald, Robarts Research Institute, University of Western Ontario, London, ON N6A 3K7, Canada.
E-mail: jronald@robarts.ca

Published by Elsevier Inc. on behalf of The American Society of Gene and Cell Therapy.
This is an open access article under the CC BY-NC-ND license (http://creativecommons.org/licenses/by-nc-nd/4.0/).

delivery of BEs to target tissues. Non-viral delivery methods are gaining attention due to their versatility and improved safety profile compared to viral vectors, such as adeno-associated viruses.[21,22] However, most non-viral delivery vectors suffer from low efficiency of gene transfer when compared to viral vectors. Minicircles (MCs) emerge as a potential solution to this delivery challenge. These small circular DNA vectors, derived from "parental plasmids" (PPs), lack the bacterial backbone (an antibiotic resistance gene and origin of replication) normally found in plasmids. The smaller size of MCs allows for higher transfection and transgene expression compared to plasmids.[23,24] Additionally, the absence of bacterial components reduces potential immune responses and eliminates the transfer of antibiotic genes to mammalian hosts.[25,26] Thus, the attributes of MCs could allow for efficient and safe delivery of BEs, but, to our knowledge, studies exploring this have not been described.

As BEs and delivery methods continue to advance, it becomes crucial to accurately assess the efficiency of these technologies in cells and animal models prior to translation into patients. While current evaluation methods, such as next-generation sequencing and immunohistochemistry for proteins of interest, offer valuable bulk information about base editing activity, they often require cell (or animal) death and lack spatial and kinetic details required at both the single-cell and whole-animal scale.[12,14] In 2020, Katti et al. introduced the "Gene On" (GO) optical reporter systems to allow for indirect visualization of base editing activity in live cells.[27] For ABE evaluation, the reporter genes were mutated to contain a premature TAG stop codon, which only produces imaging protein and signal when edited to TGG (tryptophan codon) by an ABE. Similarly, for CBE evaluation, reporter genes were mutated to modify their ATG start codon to ACG, allowing imaging protein production only when edited to ATG methionine by a CBE. Fluorescence-based GO systems utilize mutated versions of green fluorescent protein (GFP), called GFP^{GO}, which can be corrected and activated in the presence of CBEs or ABEs and respective sgRNAs, enabling quantification of edited cells using flow cytometry. Additionally, this group described a bioluminescence version of the GO system using firefly luciferase, termed LUC^{GO}. This GO system provides measurements from bulk cell populations in culture. In this study, we adopted the original LUC^{GO} system and built a second GO system using Akaluciferase (Akaluc), termed Akaluc^{GO}. Akaluc is an optimized firefly luciferase mutant that uses Akalumine-hydrochloride to produce light peaking at 650 nm.[28] Akaluc bioluminescence has demonstrated exceptional efficacy in visualizing engineered cells, even at the single-cell level, within deep tissues of mice.[29]

This study focused on *in vitro* evaluation of MCs as an alternative non-viral delivery vector for BEs using various GO systems. Specifically, we compared the editing efficiency of MC-based ABE and CBE editing to that of their PP counterparts in cancer cells stably expressing a GFP^{GO} reporter, LUC^{GO} reporter, or Akaluc^{GO} reporter, the latter of which was constructed in this study. This investigation provides novel insights into the potential of MCs as a safe and efficient delivery platform for base editing in various cellular contexts, moving us closer to harnessing the full potential of genome editing technologies.

RESULTS

2-Plasmid ABE + sgRNA delivery using GFP^{GO}

We first validated the ABE GFP^{GO} reporter system previously developed by Katti et al. (Figure 1A).[27] HEK293T cells were engineered to express ABE GFP^{GO} and then transfected with a plasmid encoding sgRNA and tdTomato (sgRNA-tdT) and a separate plasmid encoding either ABE or Cas9n as a negative control (Figure 1B). After 48 h, tdT expression was observed from both groups, indicating successful transfection of sgRNA-encoding plasmid (Figure 1C). GFP expression was observed in cells transfected with ABE, while cells transfected with Cas9n exhibited minimal GFP expression. Analysis using flow cytometry showed that a significantly higher 42% of tdT-positive cells were also GFP-positive when transfected with ABE compared to Cas9n (Figure 1D; $p < 0.001$). Time-lapse microscopy qualitatively showed tdT fluorescence beginning ~9 h post transfection and GFP fluorescence beginning ~12 h post transfection (Figure 1E). The number of green objects appeared to reach the number of red objects by 48h. This may be due to proliferation of edited GFP-positive cells while the sgRNA-tdT plasmid is diluted with cell division (Figure 1E).

All-in-one PP/MC ABE + sgRNA using GFP^{GO}

To facilitate the delivery of sgRNA and ABE within a single vector, as would likely be done in patients, we designed PPs encoding ABE or Cas9n and the appropriate sgRNA (Figure 1F). In the production of MCs from PPs, the addition of arabinose induces the expression of both phi-C31 integrase and I-SceI endonuclease. This initiates a recombination process between attB and attP sites within the MC, followed by the endonuclease-mediated degradation of the plasmid backbone. This process excises everything but the expression cassette to allow isolation of the desired MC DNA. MCs were produced, and construct sizes were confirmed with gel electrophoresis (Figure 1G). ABE GFP^{GO}-expressing HEK293T cells were transfected with PPs or MCs, and GFP was apparent in fluorescent microscopy images using ABE, but not Cas9n, vectors (Figure 1H). Flow cytometry analysis indicated that both PP and MC transfections yielded a significantly higher proportion of GFP-positive cells compared to Cas9n controls (Figure 1I; $p < 0.0001$). Additionally, MCs led to a higher number of GFP-positive cells compared to PPs ($p < 0.01$).

All-in-one PP/MC CBE + sgRNA using GFP^{GO}

The CBE GFP^{GO} reporter was engineered to co-express a constitutive mScarlet to aid in cell sorting (Figure 2A). We also switched to a cancer cell line (HeLa) that could potentially be used in a preclinical tumor model. HeLa cells were engineered with CBE GFP^{GO} and sorted for low, medium, and high levels of mScarlet expression (Figure S1A). A low percentage (1.8%) of cells with high mScarlet expression also expressed GFP (Figure S1B), so medium sorted cells were used in all subsequent experiments. Like our all-in-one ABE PPs, we constructed all-in-one CBE PPs co-expressing the appropriate sgRNA and generated PPs and MCs of the appropriate size (Figures 2B and

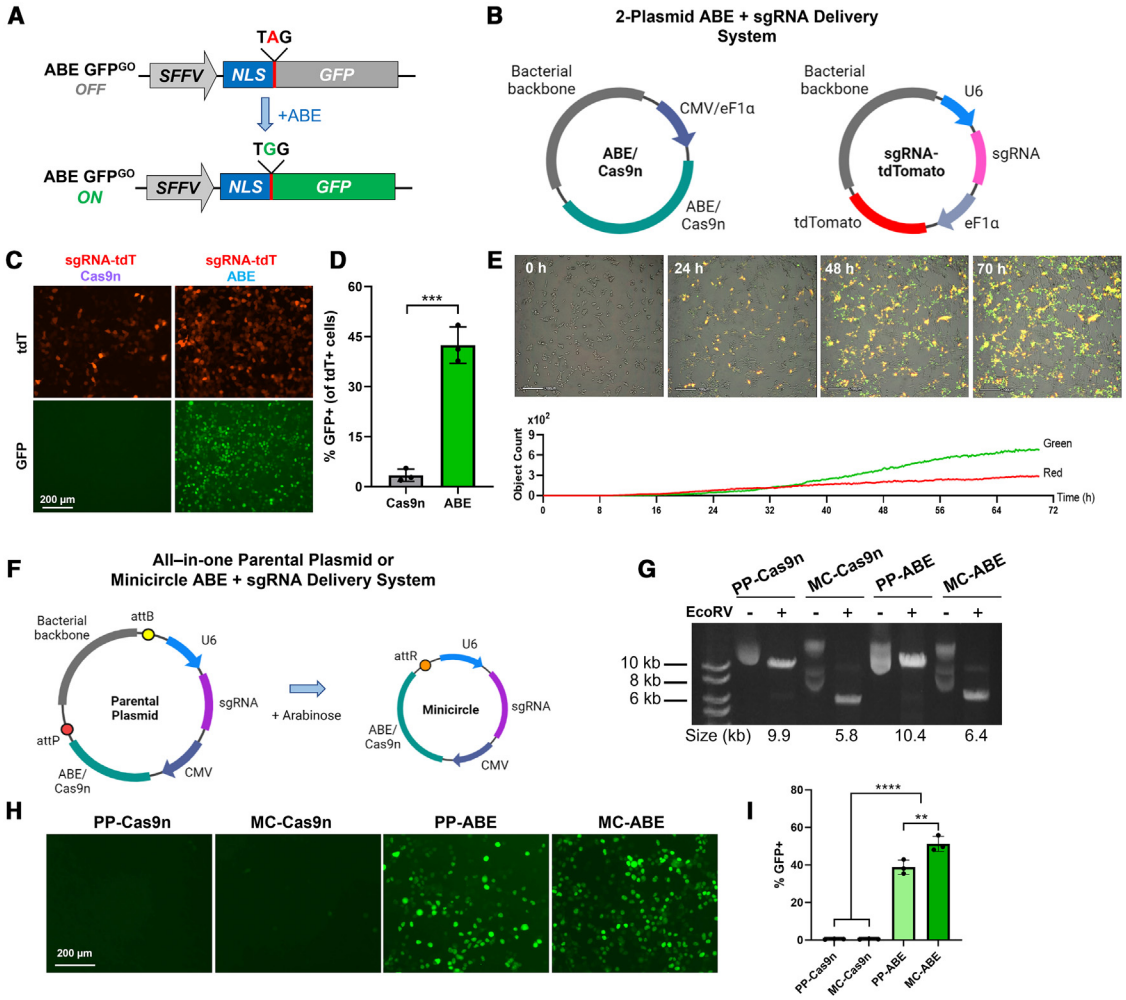

Figure 1. 2-Plasmid and all-in-one PP/MC ABE + sgRNA delivery using GFP^{GO}

(A) Schematic of the ABE GFP^{GO} reporter. Insertion of a premature stop codon (TAG) after the nuclear localization signal prevents full-length functional GFP expression. Editing of A > G at the stop codon by the adenine BE (ABE) complexed with single-guide RNA (sgRNA) enables full-length expression of GFP. (B) Utilization of a 2-plasmid system, with one delivering sgRNA with tdTomato (sgRNA-tdT) and the second delivering ABE or Cas9n as a negative control. (C) Fluorescence microscopy of HEK293T-GFP^{GO} cells 48 h after transfection with sgRNA-tdT and ABE or Cas9n. (D) Flow cytometry analysis of cells 48 h after transfection, indicating the percentage of tdT-expressing cells that also exhibit GFP expression ($n = 3$). (E) Live-cell imaging and counts of tdT and GFP expression over time following transfection with sgRNA-tdT and ABE plasmids. (F) All-in-one delivery system combining the sgRNA and ABE or Cas9n into a single DNA delivery vector. Parental plasmids (PPs) containing attB and attP sites undergo recombination upon arabinose induction, resulting in the production of minicircles (MCs) free of bacterial DNA components. (G) Agarose gel electrophoresis following EcoRV restriction digestion, confirming production of PPs and MCs expressing Cas9n or ABE. (H) Fluorescence microscopy of HEK293T-GFP^{GO} cells 48 h after transfection with PP-Cas9n, MC-Cas9n, PP-ABE, or MC-ABE. (I) Flow cytometry analysis of cells 48 h after transfection ($n = 3$). Data are presented as mean ± SD (**$p < 0.01$, ***$p < 0.001$, ****$p < 0.0001$).

2C). CBE GFP^{GO}-expressing HeLa cells were transfected with PPs or MCs and flow cytometry demonstrated a significantly higher percentage of GFP-positive cells following MC transfection compared to both PP and Cas9n controls (Figure 2D; $p < 0.0001$). Additionally, PPs expressing CBE exhibited a significantly higher proportion of GFP-positive cells when compared to PP and MC Cas9n controls (Figure 2D; $p < 0.001$). Time-lapse microscopy revealed that the number of GFP-positive cells seemed to plateau 60 h after transfection for PPs but, using MCs, continued to increase up to 72 h (Figures 2E and 2F). Longitudinal flow cytometry data showed that the percentage of GFP-positive GFP^{GO} cells after MC CBE delivery peaked at day 5 and remained constant until our last measurement point at day 18 (Figure S2).

All-in-one PP/MC ABE + sgRNA using Akaluc^{GO}

To expand the GO system to allow bioluminescence imaging of ABE activity, we incorporated Akaluc, a highly sensitive luciferase with red-shifted emission, into two separate GO systems. In our first

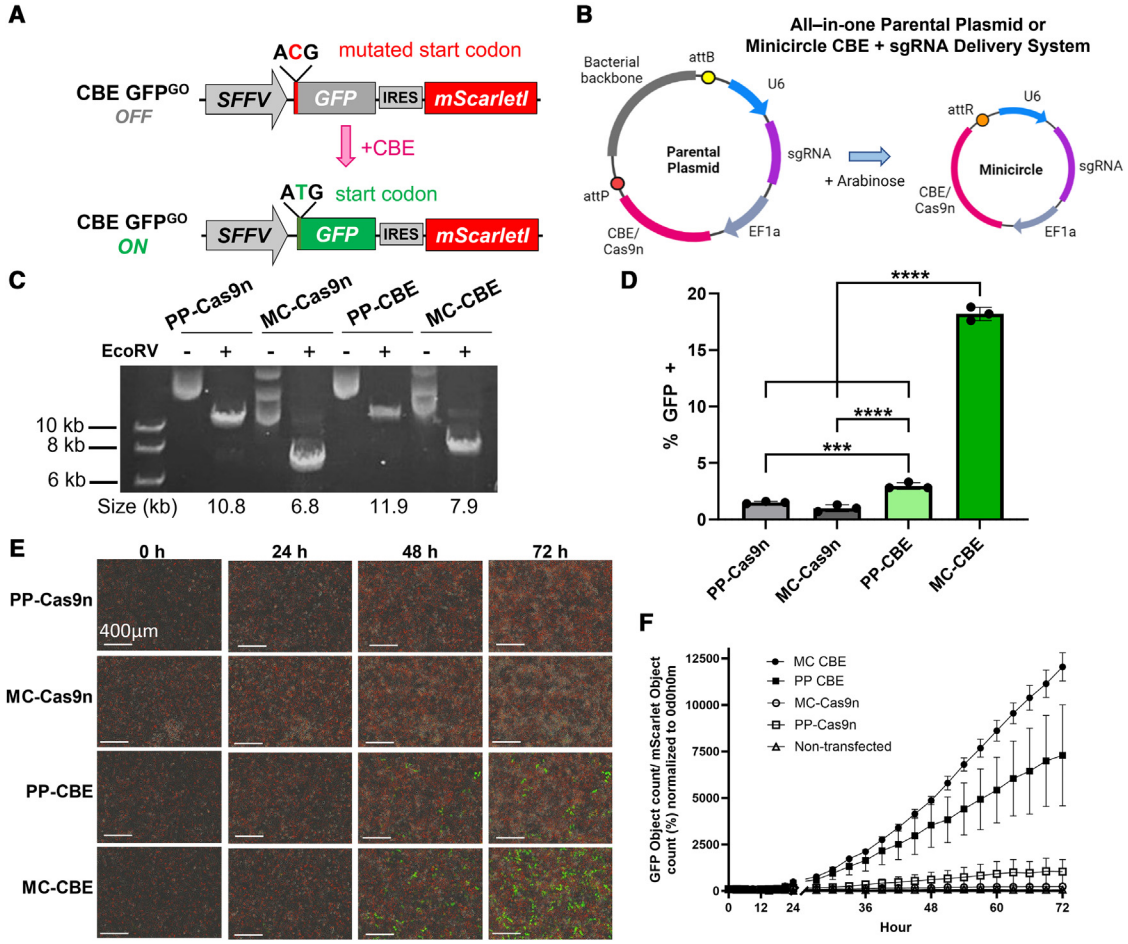

Figure 2. All-in-one PP/MC CBE + sgRNA using GFP^{GO}

(A) Schematic of the CBE GFP^{GO} reporter. GFP expression is inactivated by a mutation of the protein start codon (ATG to ACG). C > T editing at the mutated start codon by CBE complexed with the sgRNA enables expression of GFP. (B) PP encoding the sgRNA and CBE sequences for single DNA vector delivery. (C) Restriction digestion using EcoRV and agarose gel electrophoresis of PPs and MCs expressing Cas9n or CBE to confirm vector size. (D) Flow cytometry analysis of HeLa cells stably expressing medium mScarletI-GFP^{GO} 48 h after transfection for percent of GFP-positive cells ($n = 3$). (E) Fluorescence microscopy of cells 48 h after transfection with PP or MC with CBE or Cas9n control vectors. (F) Incucyte counts of GFP object count/mScarlet object count over 72 h. At each time point, 19 images were captured per well, for each PP and MC test. The average value was then calculated for each well and time point ($n = 3$). Data are presented as mean ± SD (***$p < 0.001$, ****$p < 0.0001$).

iteration, which we named ABE [GFP-Akaluc]^{GO}, we cloned Akaluc downstream of the mutated GFP transgene in the ABE GFP^{GO} construct and separated these two transgenes by a T2A self-cleaving peptide sequence (Figure S3A). As the Akaluc sequence does not have an independent start codon, we theorized that Akaluc expression would only be present in cells following ABE-mediated editing of the premature stop codon in GFP. We use a lentivirus to engineer HeLa cells to stably express the ABE [GFP-Akaluc]^{GO} system. These cells were then transfected with PP-ABE or PP-Cas9n. After 48 h, GFP expression was only visible in cells transfected with PP-ABE (Figure S3B). Bioluminescence imaging revealed that the highest signal was in cells transfected with PP-ABE, but an unexpectedly high level of background signal was seen in cells transfected with PP-Cas9n (Figures S3C and S3D; $p < 0.001$).

To address this background signal, we engineered a second Akaluc GO system, which we called Akaluc^{GO}. We hypothesized that the background issue may be partially attributable to non-canonical translation initiation of Akaluc, so in Akaluc^{GO} we expressed tdT constitutively upstream of a mutated Akaluc containing a premature stop codon (separated by a P2A linker; Figure 3A).[30] We then redesigned all-in-one PPs and MCs to contain a sgRNA targeting this premature stop codon. HeLa cells were engineered with the Akaluc^{GO} lentivirus, sorted for various levels of tdT expression (low, medium, high; Figure S4A), and transfected with PPs or MCs expressing ABE or Cas9n. After 48 h, cells transfected with MCs expressing Cas9n showed minimal Akaluc signal in the cells sorted for low and medium tdT levels (Figures S4B and S4C). However, significant background was seen in cells sorted for high tdT expression. Thus, for the rest of

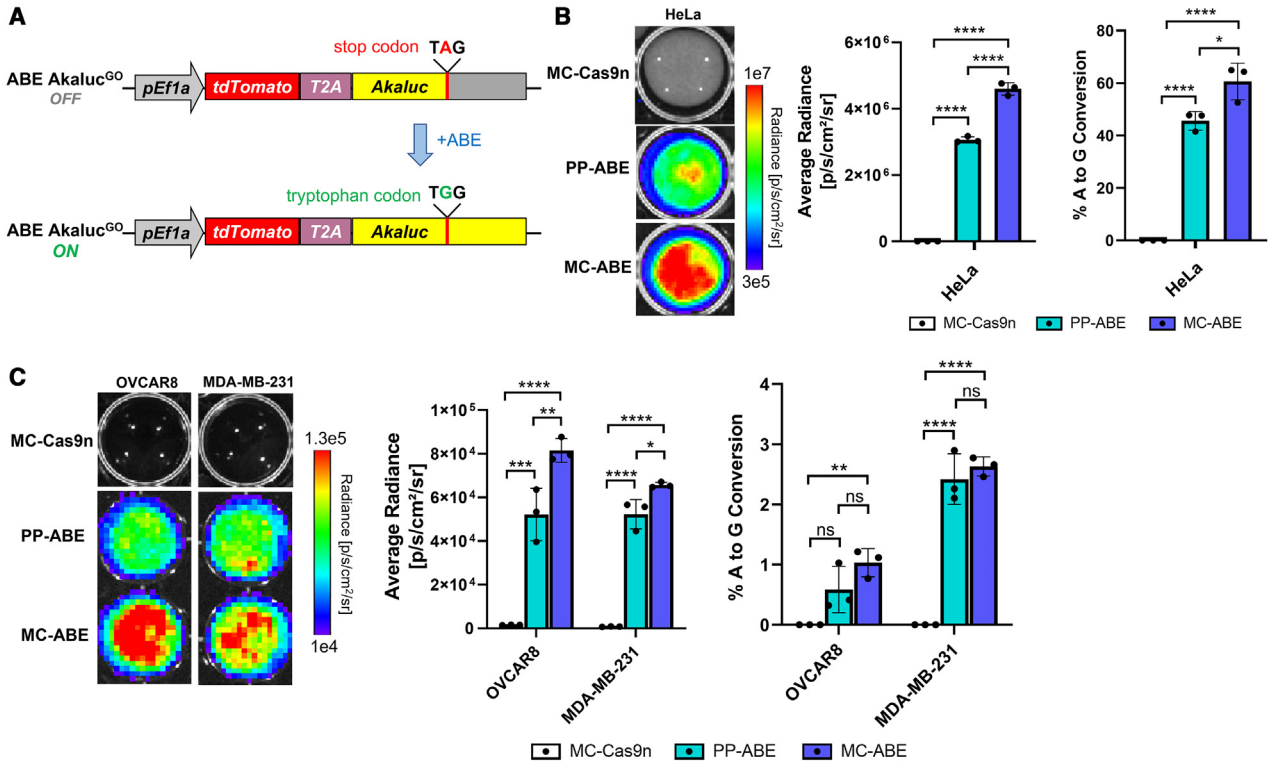

Figure 3. All-in-one PP/MC ABE + sgRNA using Akaluc^{GO}

(A) Schematic of the Akaluc^{GO} reporter. A > G editing of the stop codon by ABE enables full-length expression of Akaluc. (B and C) tdT-Akaluc^{GO}-expressing (B) HeLa cells or (C) OVCAR8 and MDA-MB-231 cells 48 h after transfection with MC expressing ABE or Cas9 and PP expressing ABE. Also shown are quantification of the average radiance of cells at 48 h ($n = 3$) and sequencing data showing the percentage of A-to-G conversion in ABE Akaluc^{GO} cells and percent editing at the target site in HeLa, MDA-MB-231, and OVCAR8 Akaluc^{GO} cells (medium tdT expression) as quantified by BEAT analysis of Sanger sequencing ($n = 3$). Data are presented as mean ± SD (ns, non-significant; $^{*}p < 0.05$, $^{**}p < 0.01$, $^{***}p < 0.001$, $^{****}p < 0.0001$).

our study, all cancer cells engineered with the Akaluc^{GO} lentivirus were sorted for a medium level of tdT expression to minimize background. However, it is important for the luciferase GO systems to not compare absolute bioluminescent signal across cell types, as we did not account for differences in GO system reporter copy number.

For all cell types, transfection with MCs expressing ABE resulted in a significantly higher Akaluc signal compared to PPs (Figures 3B and 3C; $p < 0.05$). Additionally, with MC ABE delivery, the signal-to-noise ratios (SNRs) were 304.2, 40.7, and 50.2 for HeLa, 231, and OVCAR8 cells, respectively, while under PP ABE, the corresponding SNRs were 202.6, 20.5, and 31.8. Based on Base Editing Analysis Tool (BEAT) analysis of Sanger sequencing, the average A-to-G conversion for HeLa cells was 45.6% ± 3.6% and 60.6% ± 7.0% for PP and MC delivery of ABE, respectively (Figure 3B; $p < 0.05$). However, for OVCAR8 and MDA-MB-231 cells, A-to-G conversion was less than 3%, and no significant differences were observed between editing with PP and MC (Figure 3C).

All-in-one PP/MC CBE + sgRNA using LUC^{GO}

Finally, to further evaluate our MC CBE constructs, we used the LUC^{GO} system previously developed by Katti et al. (Figure 4A).[27] LUC^{GO}-expressing HeLa and OVCAR8 cells were transfected with all-in-one PP or MC encoding CBE (or Cas9n) and an appropriate sgRNA. In OVCAR8 cells, there was no difference in luciferase signal between PP and MCs encoding CBE, but significantly higher signal for both CBE constructs compared to MCs encoding Cas9n (Figure 4B). Likewise, in alignment with the Akaluc^{GO} ABE system, there was no significant difference observed in C-to-T conversion for OVCAR8 cells with PP-CBE or MC-CBE delivery, with an average conversion rate of less than 2% (Figure 4B). For HeLa cells, images showed significantly increased luciferase signal in HeLa cells using MCs encoding CBE versus MCs encoding Cas9n and PPs encoding CBE (Figure 4C). The average C-to-T conversion rate in HeLa cells was 5.2% ± 3.8% for PP CBE and 11.60% ± 1.8% for MC CBE (Figure 4C; $p < 0.05$). The SNRs with MC CBE delivery were 7.3 and 39.7 for HeLa and OVCAR8 cells respectively, while under PP CBE, the corresponding SNRs were 1.5 and 35.4.

DISCUSSION

Base editing represents a versatile genome editing tool and promising avenue to treat thousands of genetic disorders. However, the clinical application of this technology hinges on the development of both safe

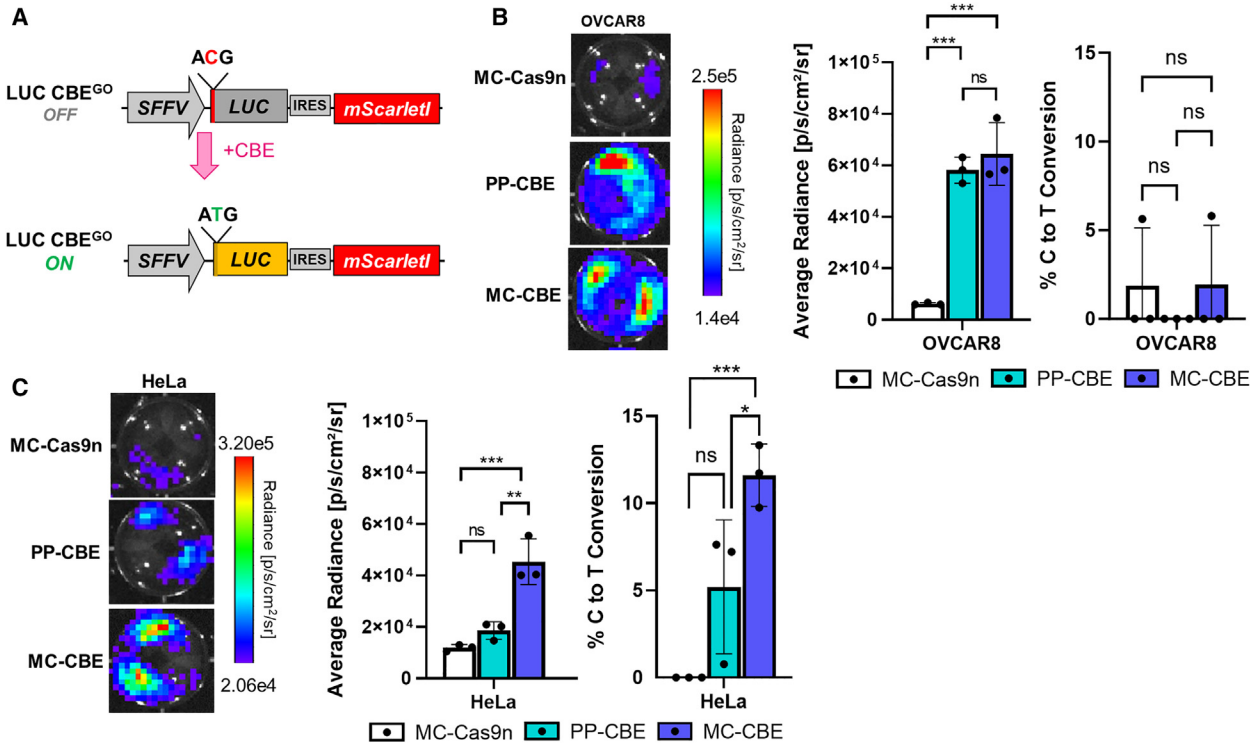

Figure 4. All-in-one PP/MC CBE + sgRNA using LUC^{GO}

(A) Schematic of the LUC^{GO} reporter. C > T editing at the mutated start codon by CBE complexed with sgRNA enables the expression of LUC. (B and C) Bioluminescence imaging of LUC^{GO} expressing (B) OVCAR8 or (C) HeLa cells 48 h after transfection with MC expressing CBE or Cas9 and PP expressing CBE. Also shown are quantification of the average radiance of cells at 48 h (n = 3) and sequencing data showing the percentage of C-to-T editing at the target site in CBE LUC^{GO} HeLa and OVCAR8 cells (medium mScarlet expression) as quantified by BEAT analysis of Sanger sequencing (n = 3). Data are presented as mean ± SD (ns, $^{*}p < 0.05$, $^{**}p < 0.01$, $^{***}p < 0.001$).

and efficient delivery mechanisms for BEs within target tissues. MCs present several advantages over traditional BE delivery vectors such as plasmids, mRNA, and adeno-associated virus. These advantages include enhanced transgene expression, reduced immunogenicity, and simplified production processes. In this study, we investigate the potential of DNA MCs as an innovative non-viral vector for delivering ABEs and CBEs, aiming to overcome the limitations associated with conventional delivery vectors and enhance the clinical applicability of base editing technology.

After testing the functionality of the ABE GFP^{GO} system, we noted that the GFP fluorescence began approximately 12 h after transfection, indicating a time lag between delivery of ABE vectors and GFP activation. Next, creating an all-in-one PP and MC was done with the goal of a system that could be used in a therapeutic setting. In both the ABE and CBE systems for GFP^{GO}, there was a significant increase in MCs over PPs. These results align with previous studies demonstrating higher transgene expression using MCs compared to plasmids both *in vitro* and *in vivo*.[23,24,31,32] The improved transgene expression is likely due to the smaller size of our MCs (~61.5% the size of PPs). Prior research has shown an inverse relationship between vector size and transgene expression levels,[33,34] with larger vectors exhibiting limited diffusion into the nucleus during the multi-step transfection process, resulting in lower transgene expression.[35] Since the mass of transfection agents is the primary safety limitation, a main advantage of MCs is that more moles of vector can be delivered compared to PPs at a given mass of agent. In our studies, as equal masses of MC and PP were transfected, cells were exposed to ~1.6 times more copies of the ABE and CBE transgene.

Beyond 72 h, we see that the GFP^{GO} signal plateaus at day 5 with CBE. This observation suggests that BE activity is complete, but if the scope of this work is to be expanded beyond the highly proliferative cancer cells used in this study, then, in contrast with somatic non-dividing tissues, there should be consideration made for alternative strategies of regulating BE expression.[23,36,37] While MCs have been proven to enhance base editing levels *in vitro* compared to plasmids, they also sustain transgene expression longer in non-dividing cells. This may not be ideal for BE delivery, especially considering the higher off-target editing associated with plasmid delivery compared to mRNA or ribonucleoprotein methods.[38,39] We will investigate off-target editing with MCs versus plasmids in future studies. This also underscores the importance of exploring regulatory mechanisms for controlling BE expression, such as driving expression using inducible promoters.

Notably, previous work by Song et al. demonstrated that plasmids encoding ABE did not induce off-target editing *in vivo*, which highlights the need for further scrutiny in our own work to see whether there is a difference with MCs.[14]

Developing an *in vivo* compatible reporter system for non-invasive tracking of ABE activity, we had two iterations, the first [GFP-Akaluc]^{GO} system having unexpected Akaluc background signal in the absence of ABE. For our second iteration, [tdt-Akaluc]^{GO}, we were able to significantly reduce the background signal by introducing a premature stop codon, which minimizes the potential of alternative in-frame start codons or translation re-initiation.[40–43] Interestingly, cells sorted for high mScarlet or tdT expression levels of the GFP^{GO} CBE systems and the [tdt-Akaluc]^{GO} ABE systems had higher GFP or Akaluc background expression, likely from stop-codon readthrough or alternative start sites.[44–49] These results demonstrate that engineering cells to strongly express an activatable reporter may not always be favorable and that balancing strong activation with background expression may be necessary.

Studying the MC delivery and activation of the bioluminescent reporters Akaluc^{GO} and LUC^{GO}, we found varying levels of activation between HeLa, OVCAR8, and MDA-MB-231 cells, corresponding to varying SNRs. In all types, we found a significant increase in bioluminescent signal from MC-ABE or MC-CBE over MC-Cas9n, whereas with Sanger sequencing, we were only able to detect a significant change in the HeLa cells. All cell types had SNR values above 5 and displayed visually discernible contrast upon both MC and PP BE delivery, except for HeLa cells with PP CBE delivery. Activation of LUC^{GO} was detectable with bioluminescent signal but not with Sanger sequencing of genomic PCR products. One plausible explanation for this is that the genome may only contain one or few copies of the LUC^{GO} gene, but activation of these transgene(s) can produce many copies of the enzyme, which can catalyze multiple luciferin substrates, to facilitate amplified sensitive detection of bioluminescence signal. With ABEs for MDA-MB-231 and OVCAR8, we saw low A-to-G conversion (<3%), which can likely be attributed to their lower transfection efficiency compared to HeLa cells[33,50] as well as potential differences in cell repair pathways, which is required for base conversion.[51–53] These results underscore the sensitivity of the Akaluc^{GO} system in detecting even low levels of base editing, which highlights its potential as a powerful tool for monitoring ABE activity *in vitro* and for comparing the efficiency of different ABE delivery vectors.

There are some limitations to our Akaluc^{GO} reporter system, which necessitates further exploration and optimization. First, the background signal could be further reduced, either by sorting the cells for a lower level of tdT or by optimizing the location of the premature stop codon within the Akaluc gene. Second, while Akaluc has been engineered to emit red-shifted light for improved tissue penetration, its sensitivity may still be limited in deep tissues and larger animal models due to substrate and oxygen availability, making it difficult to accurately assess Akaluc expression in deep-seated solid tumors.

In conclusion, this study pioneers the use of MCs as a promising vector for efficient ABE and CBE delivery across multiple cancer cell types *in vitro*. Additionally, we developed Akaluc^{GO} as a highly responsive bioluminescence reporter system for visualizing adenine base editing. We showed that LUC^{GO} and Akaluc^{GO} can detect *in vitro* ABE or CBE activity in cells with high sensitivity and specificity. Future work will further optimize the LUC^{GO} and Akaluc^{GO} reporter systems to reduce background signals for *in vivo* testing and extend their application to other tumor models, such as lung and liver, for organ-specific adenine and cytosine base editing tracking. Moreover, our exploration will encompass new genomic disease targets, new GO reporters, and alternative ABE/CBE delivery strategies to further expand the genome editing toolbox for genetic disease treatment.

MATERIALS AND METHODS

Cell lines

HEK293T cells, HeLa cervical cancer cells, MDA-MB-231 breast cancer cells, and OVCAR8 ovarian cancer cells were obtained from the American Type Culture Collection (VA, USA). Cells were cultured in DMEM (HEK293T, HeLa, and MDA-MB-231 cells) or RPMI (OVCAR8) supplemented with 10% fetal bovine serum and 5% (v/v) antibiotic-antimycotic at 37°C and 5% CO_2. All cells were routinely verified as free of mycoplasma contamination using the MycoAlert Mycoplasma Detection Kit (Lonza, NY, USA).

GO reporter system lentiviral constructs

Lentiviral transfer plasmids encoding the original GFP^{GO} and LUC^{GO} systems were gifts from Lukas Dow (Addgene plasmids): pRRL-GFPAdGO2-PGK-Neo (ABE GFP^{GO}; Figure 1A; 136899), pRRL-mU6-sgGO-SFFV-GFP^{GO}-IRES-mScarletI (CBE GFP^{GO}; Figure 2A; 136895), and pRRL-mU6-sgGO-SFFV-LUC2^{GO} (CBE LUC^{GO}; Figure 4A; 136905).[27] The CBE GFP^{GO} and CBE LUC^{GO} plasmids were modified to remove the sgRNAs (called sgGO in the original constructs). Additionally, an IRES-mScarletI fragment was cloned into the CBE LUC^{GO} plasmid downstream of the LUC^{GO} sequence.

Two ABE-targeted GO systems encoding Akaluc were made. An ABE [GFP-Akaluc]^{GO} (Figure S3A) lentiviral transfer plasmid was made by amplifying a T2A-Akaluc fragment from LV-pEF1α-tdT-Akaluc[54] and inserting it downstream of GFP^{GO} in the ABE GFP^{GO} construct using In-Fusion HD Cloning (Takara Bio, CA, USA). In addition, using an LV-pEF1α-tdT-Akaluc plasmid, an ABE Akaluc^{GO} lentiviral transfer plasmid (Figure 3A) with constitutive tdT expression was generated by incorporating an ATG-to-TAG mutation at the 265th amino acid position within Akaluc using the Q5 Site-Directed Mutagenesis Kit (New England Biolabs, MA, USA). The optimal site to insert the premature stop codon into Akaluc was determined using Benchling's CRISPR guide design feature (www.benchling.com/crispr), where the sgRNA with the highest specificity and efficiency score was selected to allow an A-to-G conversion within the ABE8e editing window (positions 4–8).[55]

Lentiviral production and cell engineering

As described previously,[56] third-generation lentiviral vectors were produced using packaging and envelope expression plasmids (kind gifts from Didier Trono; pMDLg/pRRE, pRSV-Rev, and pMD2.G; Addgene plasmids 12251, 12253, and 12259, respectively).[57] Various cancer cell lines were transduced using these vectors, as described previously.[27] Cells engineered to express ABE GFP^{GO} or ABE $[GFP\text{-}Akaluc]^{GO}$ were selected with 400 μg/mL Geneticin for 7–10 days. Cells engineered with LUC^{GO}, $Akaluc^{GO}$, and CBE GFP^{GO} vectors were sorted for constitutive tdT (ABE) or mScarletI (CBE) expression using a FACSAria III fluorescence-activated cell sorter (BD Biosciences, CA, USA).

2-Plasmid BE system

Our initial experiments involved delivery of the BE and sgRNA into cells using two separate plasmids. A plasmid encoding an efficient ABE (ABE8e(TadA-8e V106W)) was a gift from David Liu (Figure 1B; Addgene plasmid 138495).[58] A plasmid containing a sgRNA specific for ABE GFP^{GO} with constitutive tdT (sgRNA-tdT) was a gift from Lukas Dow (Figure 1B; Addgene plasmid 136911).[27] As a control Cas9n plasmid, we cloned a high-fidelity Cas9n fragment from an FNLS-HiFi plasmid into a pLenti-Cas9-P2A-Puro backbone (Addgene plasmids 136902 and 110837, respectively).[27,59]

All-in-one PP and MC BE systems

To generate different "all-in-one" PPs expressing either ABE8e (Figure 1F) or CBE (Figure 2B) along with the appropriate sgRNAs, the vector PP-pSurvivin-SEAP[23] was used. Briefly, the pSurvivin-SEAP expression cassette was replaced with ABE from ABE8e (TadA-8e V106W) or CBE from FNLS-HiFi. ABE or CBE was driven either by the CMV or EF1a promoter, respectively. A control PP encoding Cas9n was generated by deleting the adenine deaminase domain or the cytosine deaminase domain. Additionally, U6 promoter-driven sgRNAs of interest were cloned into PPs (Table S1 contains the protospacer sequences for sgRNAs of interest). MCs expressing ABE, CBE, and Cas9n were generated using the MC-Easy Minicircle DNA Production Kit (System Biosciences, CA, USA).[60]

Cell transfection and GO reporter assays

Cells stably expressing the GO systems were transfected with the various BE or control systems (2-plasmid or all-in-one PP or MC) using jetPEI (Polyplus Transfection, PA, USA) or Lipofectamine 3000 (Thermo Fisher Scientific). For GFP^{GO} systems, fluorescence reporter expression was visualized using an EVOS FL Auto Imaging System (Thermo Fisher Scientific) or Revolve 4 ECHO microscope (ECHO, CA, USA). Fluorescence was also evaluated via flow cytometry using a BD FACSCanto flow cytometer and FlowJo software (BD Biosciences). For some constructs, fluorescence microscopy images were also taken immediately following transfection and subsequently at 10-min intervals for up to 70 h using a CytoSMART Lux3 FL incubator microscope (CytoSMART Technologies, AZ Eindhoven, the Netherlands). Additional kinetic studies were carried out using the Incucyte Live-Cell Analysis System (Sartorious, Göttingen, Germany).

For $Akaluc^{GO}$ and LUC^{GO} systems, images were taken using the IVIS Lumina XRMS In Vivo Imaging System after addition of 5 μL of 30 mg/mL D-Luciferin or 5 mM Akalumine-HCl, respectively (PerkinElmer, MA, USA). Regions of interest were manually delineated around wells using LivingImage software to measure bioluminescence average radiance ($p/s/cm^2/sr$). The SNR was calculated by taking the mean signal in wells that received BEs minus the mean signal in wells receiving Cas9n vectors (control) divided the mean standard deviation of the background.

Sequencing analysis

To further analyze ABE and CBE editing, genomic DNA was extracted from the cells 48 h after transfection using the DNeasy Blood and Tissue Kit (QIAGEN, CA, USA). The GFP^{GO}, LUC^{GO}, and $Akaluc^{GO}$ target sites were amplified by PCR using primers that bind approximately 200 bp upstream and downstream of the target A or C (Table S2). The PCR products were then purified using the QIAquick PCR Purification Kit (QIAGEN, CA, USA), and analyzed by Sanger sequencing. BEAT (http://www.hanlab.cc/beat) was used to quantify base editing from Sanger sequencing data.[61]

Statistics

Statistical tests were performed using GraphPad Prism software (v.8.1.2 for Mac OS X, GraphPad, CA, USA, www.graphpad.com). An unpaired two-tailed t test was performed to compare GFP^{GO}, $Akaluc^{GO}$ and LUC^{GO} activation between two groups. Ordinary one-way ANOVA and Tukey's multiple comparison post hoc test were used to compare GFP^{GO}, $Akaluc^{GO}$, and LUC^{GO} activation from PP and MC delivery of ABE, CBE, or Cas9n. All experiments were performed in triplicate wells for each condition unless otherwise stated. A p value less than 0.05 was considered statistically significant.

DATA AND CODE AVAILABILITY

The data underlying this article will be shared on reasonable request to the corresponding author.

SUPPLEMENTAL INFORMATION

Supplemental information can be found online at https://doi.org/10.1016/j.omtn.2024.102248.

ACKNOWLEDGMENTS

This work was supported by a Natural Sciences and Engineering Research Council of Canada Discovery Grant (RGPIN-2016-05420 to J.A.R.). This work was funded in part by a Canada Graduate Doctoral Scholarship from the Natural Sciences and Engineering Research Council of Canada of Canada (to M.M.E.) and a Canadian Institute for Health Research Canadian Graduate Scholarship Masters Award (to S.L.).

AUTHOR CONTRIBUTIONS

M.M.E., S.L., and J.A.R. designed the research. M.M.E., S.L., J.S.K., C.G.S., and R.L. performed the research. M.M.E., S.L., C.G.S., and J.A.R. analyzed data. J.A.R. provided supervision. M.M.E., S.L., and J.A.R. wrote the paper.

DECLARATION OF INTERESTS

The authors declare no competing interests.

REFERENCES

1. Mahdieh, N., and Rabbani, B. (2013). An Overview of Mutation Detection Methods in Genetic Disorders. Iran. J. Pediatr. *23*, 375–388.
2. Stephens, P.J., Tarpey, P.S., Davies, H., Van Loo, P., Greenman, C., Wedge, D.C., Nik-Zainal, S., Martin, S., Varela, I., Bignell, G.R., et al. (2012). The landscape of cancer genes and mutational processes in breast cancer. Nature *486*, 400–404. https://doi.org/10.1038/nature11017.
3. Nowak, K.J., and Davies, K.E. (2004). Duchenne muscular dystrophy and dystrophin: pathogenesis and opportunities for treatment. EMBO Rep. *5*, 872–876. https://doi.org/10.1038/sj.embor.7400221.
4. Landrum, M.J., Lee, J.M., Benson, M., Brown, G., Chao, C., Chitipiralla, S., Gu, B., Hart, J., Hoffman, D., Hoover, J., et al. (2016). ClinVar: public archive of interpretations of clinically relevant variants. Nucleic Acids Res. *44*, D862–D868. https://doi.org/10.1093/nar/gkv1222.
5. Landrum, M.J., Lee, J.M., Riley, G.R., Jang, W., Rubinstein, W.S., Church, D.M., and Maglott, D.R. (2014). ClinVar: public archive of relationships among sequence variation and human phenotype. Nucleic Acids Res. *42*, D980–D985. https://doi.org/10.1093/nar/gkt1113.
6. Ran, F.A., Hsu, P.D., Wright, J., Agarwala, V., Scott, D.A., and Zhang, F. (2013). Genome engineering using the CRISPR-Cas9 system. Nat. Protoc. *8*, 2281–2308. https://doi.org/10.1038/nprot.2013.143.
7. Gostimskaya, I. (2022). CRISPR–Cas9: A History of Its Discovery and Ethical Considerations of Its Use in Genome Editing. Biochemistry. *87*, 777–788. https://doi.org/10.1134/S0006297922080090.
8. Kosicki, M., Tomberg, K., and Bradley, A. (2018). Repair of double-strand breaks induced by CRISPR-Cas9 leads to large deletions and complex rearrangements. Nat. Biotechnol. *36*, 765–771. https://doi.org/10.1038/nbt.4192.
9. Komor, A.C., Kim, Y.B., Packer, M.S., Zuris, J.A., and Liu, D.R. (2016). Programmable editing of a target base in genomic DNA without double-stranded DNA cleavage. Nature *533*, 420–424. https://doi.org/10.1038/nature17946.
10. Gaudelli, N.M., Komor, A.C., Rees, H.A., Packer, M.S., Badran, A.H., Bryson, D.I., and Liu, D.R. (2017). Programmable base editing of A·T to G·C in genomic DNA without DNA cleavage. Nature *551*, 464–471. https://doi.org/10.1038/nature24644.
11. Newby, G.A., Yen, J.S., Woodard, K.J., Mayuranathan, T., Lazzarotto, C.R., Li, Y., Sheppard-Tillman, H., Porter, S.N., Yao, Y., Mayberry, K., et al. (2021). Base editing of haematopoietic stem cells rescues sickle cell disease in mice. Nature *595*, 295–302. https://doi.org/10.1038/s41586-021-03609-w.
12. Xu, L., Zhang, C., Li, H., Wang, P., Gao, Y., Mokadam, N.A., Ma, J., Arnold, W.D., and Han, R. (2021). Efficient precise in vivo base editing in adult dystrophic mice. Nat. Commun. *12*, 3719. https://doi.org/10.1038/s41467-021-23996-y.
13. Ryu, S.-M., Koo, T., Kim, K., Lim, K., Baek, G., Kim, S.-T., Kim, H.S., Kim, D.-E., Lee, H., Chung, E., and Kim, J.S. (2018). Adenine base editing in mouse embryos and an adult mouse model of Duchenne muscular dystrophy. Nat. Biotechnol. *36*, 536–539. https://doi.org/10.1038/nbt.4148.
14. Song, C.-Q., Jiang, T., Richter, M., Rhym, L.H., Koblan, L.W., Zafra, M.P., Schatoff, E.M., Doman, J.L., Cao, Y., Dow, L.E., et al. (2020). Adenine base editing in an adult mouse model of tyrosinaemia. Nat. Biomed. Eng. *4*, 125–130. https://doi.org/10.1038/s41551-019-0357-8.
15. Kim, Y., Hong, S.-A., Yu, J., Eom, J., Jang, K., Yoon, S., Hong, D.H., Seo, D., Lee, S.-N., Woo, J.-S., et al. (2021). Adenine base editing and prime editing of chemically derived hepatic progenitors rescue genetic liver disease. Cell Stem Cell *28*, 1614–1624.e5. https://doi.org/10.1016/j.stem.2021.04.010.
16. Yeh, W.-H., Shubina-Oleinik, O., Levy, J.M., Pan, B., Newby, G.A., Wornow, M., Burt, R., Chen, J.C., Holt, J.R., and Liu, D.R. (2020). In vivo base editing restores sensory transduction and transiently improves auditory function in a mouse model of recessive deafness. Sci. Transl. Med. *12*, eaay9101. https://doi.org/10.1126/scitranslmed.aay9101.
17. Yeh, W.-H., Chiang, H., Rees, H.A., Edge, A.S.B., and Liu, D.R. (2018). In vivo base editing of post-mitotic sensory cells. Nat. Commun. *9*, 2184. https://doi.org/10.1038/s41467-018-04580-3.
18. Suh, S., Choi, E.H., Leinonen, H., Foik, A.T., Newby, G.A., Yeh, W.-H., Dong, Z., Kiser, P.D., Lyon, D.C., Liu, D.R., et al. (2020). Restoration of visual function in adult mice with an inherited retinal disease via adenine base editing. Nat. Biomed. Eng. *5*, 169–178. https://doi.org/10.1038/s41551-020-00632-6.
19. Choi, E.H., Suh, S., Foik, A.T., Leinonen, H., Newby, G.A., Gao, X.D., Banskota, S., Hoang, T., Du, S.W., Dong, Z., et al. (2022). In vivo base editing rescues cone photoreceptors in a mouse model of early-onset inherited retinal degeneration. Nat. Commun. *13*, 1830. https://doi.org/10.1038/s41467-022-29490-3.
20. Killela, P.J., Reitman, Z.J., Jiao, Y., Bettegowda, C., Agrawal, N., Diaz, L.A., Friedman, A.H., Friedman, H., Gallia, G.L., Giovanella, B.C., et al. (2013). TERT promoter mutations occur frequently in gliomas and a subset of tumors derived from cells with low rates of self-renewal. Proc. Natl. Acad. Sci. USA *110*, 6021–6026. https://doi.org/10.1073/pnas.1303607110.
21. Lundstrom, K. (2018). Viral Vectors in Gene Therapy. Diseases *6*, 42. https://doi.org/10.3390/diseases6020042.
22. O'Keeffe Ahern, J., Lara-Sáez, I., Zhou, D., Murillas, R., Bonafont, J., Mencía, Á., García, M., Manzanares, D., Lynch, J., Foley, R., et al. (2022). Non-viral delivery of CRISPR–Cas9 complexes for targeted gene editing via a polymer delivery system. Gene Ther. *29*, 157–170. https://doi.org/10.1038/s41434-021-00282-6.
23. Ronald, J.A., Chuang, H.-Y., Dragulescu-Andrasi, A., Hori, S.S., and Gambhir, S.S. (2015). Detecting cancers through tumor-activatable minicircles that lead to a detectable blood biomarker. Proc. Natl. Acad. Sci. USA *112*, 3068–3073. https://doi.org/10.1073/pnas.1414156112.
24. Munye, M.M., Tagalakis, A.D., Barnes, J.L., Brown, R.E., McAnulty, R.J., Howe, S.J., and Hart, S.L. (2016). Minicircle DNA Provides Enhanced and Prolonged Transgene Expression Following Airway Gene Transfer. Sci. Rep. *6*, 23125. https://doi.org/10.1038/srep23125.
25. Bessis, N., GarciaCozar, F.J., and Boissier, M.-C. (2004). Immune responses to gene therapy vectors: influence on vector function and effector mechanisms. Gene Ther. *11*, S10–S17. https://doi.org/10.1038/sj.gt.3302364.
26. Lerminiaux, N.A., and Cameron, A.D.S. (2019). Horizontal transfer of antibiotic resistance genes in clinical environments. Can. J. Microbiol. *65*, 34–44. https://doi.org/10.1139/cjm-2018-0275.
27. Katti, A., Foronda, M., Zimmerman, J., Diaz, B., Zafra, M.P., Goswami, S., and Dow, L.E. (2020). GO: a functional reporter system to identify and enrich base editing activity. Nucleic Acids Res. *48*, 2841–2852. https://doi.org/10.1093/nar/gkaa124.
28. Liu, S., Su, Y., Lin, M.Z., and Ronald, J.A. (2021). Brightening up Biology: Advances in Luciferase Systems for in Vivo Imaging. ACS Chem. Biol. *16*, 2707–2718. https://doi.org/10.1021/acschembio.1c00549.
29. Iwano, S., Sugiyama, M., Hama, H., Watakabe, A., Hasegawa, N., Kuchimaru, T., Tanaka, K.Z., Takahashi, M., Ishida, Y., Hata, J., et al. (2018). Single-cell bioluminescence imaging of deep tissue in freely moving animals. Science *359*, 935–939. https://doi.org/10.1126/science.aaq1067.
30. Kwan, T., and Thompson, S.R. (2019). Noncanonical Translation Initiation in Eukaryotes. Cold Spring Harb. Perspect. Biol. *11*, a032672. https://doi.org/10.1101/cshperspect.a032672.
31. Huang, M., Chen, Z., Hu, S., Jia, F., Li, Z., Hoyt, G., Robbins, R.C., Kay, M.A., and Wu, J.C. (2009). Novel Minicircle Vector for Gene Therapy in Murine Myocardial Infarction. Circulation *120*, S230–S237. https://doi.org/10.1161/CIRCULATIONAHA.108.841155.
32. Cheng, C., Tang, N., Li, J., Cao, S., Zhang, T., Wei, X., and Wang, H. (2019). Bacteria-free minicircle DNA system to generate integration-free CAR-T cells. J. Med. Genet. *56*, 10–17. https://doi.org/10.1136/jmedgenet-2018-105405.
33. Campeau, P., Chapdelaine, P., Seigneurin-Venin, S., Massie, B., and Tremblay, J.P. (2001). Transfection of large plasmids in primary human myoblasts. Gene Ther. *8*, 1387–1394. https://doi.org/10.1038/sj.gt.3301532.
34. Yin, W., Xiang, P., and Li, Q. (2005). Investigations of the effect of DNA size in transient transfection assay using dual luciferase system. Anal. Biochem. *346*, 289–294. https://doi.org/10.1016/j.ab.2005.08.029.

35. Darquet, A.-M., Rangara, R., Kreiss, P., Schwartz, B., Naimi, S., Delaère, P., Crouzet, J., and Scherman, D. (1999). Minicircle: an improved DNA molecule for in vitro and in vivo gene transfer. Gene Ther. *6*, 209–218. https://doi.org/10.1038/sj.gt.3300816.

36. Wang, T., Chen, Y., and Ronald, J.A. (2019). A novel approach for assessment of prostate cancer aggressiveness using survivin-driven tumour-activatable minicircles. Gene Ther. *26*, 177–186. https://doi.org/10.1038/s41434-019-0067-6.

37. Wang, T., Chen, Y., Goodale, D., Allan, A.L., and Ronald, J.A. (2021). A survivin-driven, tumor-activatable minicircle system for prostate cancer theranostics. Mol. Ther. Oncolytics *20*, 209–219. https://doi.org/10.1016/j.omto.2021.01.007.

38. Porto, E.M., Komor, A.C., Slaymaker, I.M., and Yeo, G.W. (2020). Base editing: advances and therapeutic opportunities. Nat. Rev. Drug Discov. *19*, 839–859. https://doi.org/10.1038/s41573-020-0084-6.

39. Jang, H.-K., Jo, D.H., Lee, S.-N., Cho, C.S., Jeong, Y.K., Jung, Y., Yu, J., Kim, J.H., Woo, J.-S., and Bae, S. (2021). High-purity production and precise editing of DNA base editing ribonucleoproteins. Sci. Adv. *7*, eabg2661. https://doi.org/10.1126/sciadv.abg2661.

40. Benitez-Cantos, M.S., Yordanova, M.M., O'Connor, P.B.F., Zhdanov, A.V., Kovalchuk, S.I., Papkovsky, D.B., Andreev, D.E., and Baranov, P.V. (2020). Translation initiation downstream from annotated start codons in human mRNAs coevolves with the Kozak context. Genome Res. *30*, 974–984. https://doi.org/10.1101/gr.257352.119.

41. Kozak, M. (2001). Constraints on reinitiation of translation in mammals. Nucleic Acids Res. *29*, 5226–5232.

42. Van Damme, P., Gawron, D., Van Criekinge, W., and Menschaert, G. (2014). N-terminal Proteomics and Ribosome Profiling Provide a Comprehensive View of the Alternative Translation Initiation Landscape in Mice and Men. Mol. Cell. Proteomics *13*, 1245–1261. https://doi.org/10.1074/mcp.M113.036442.

43. Gaba, A., Wang, Z., Krishnamoorthy, T., Hinnebusch, A.G., and Sachs, M.S. (2001). Physical evidence for distinct mechanisms of translational control by upstream open reading frames. EMBO J. *20*, 6453–6463. https://doi.org/10.1093/emboj/20.22.6453.

44. Loughran, G., Chou, M.-Y., Ivanov, I.P., Jungreis, I., Kellis, M., Kiran, A.M., Baranov, P.V., and Atkins, J.F. (2014). Evidence of efficient stop codon readthrough in four mammalian genes. Nucleic Acids Res. *42*, 8928–8938. https://doi.org/10.1093/nar/gku608.

45. Hofhuis, J., Schueren, F., Nötzel, C., Lingner, T., Gärtner, J., Jahn, O., and Thoms, S. (2016). The functional readthrough extension of malate dehydrogenase reveals a modification of the genetic code. Open Biol. *6*, 160246. https://doi.org/10.1098/rsob.160246.

46. von der Haar, T., and Tuite, M.F. (2007). Regulated translational bypass of stop codons in yeast. Trends Microbiol. *15*, 78–86. https://doi.org/10.1016/j.tim.2006.12.002.

47. Wangen, J.R., and Green, R. (2020). Stop codon context influences genome-wide stimulation of termination codon readthrough by aminoglycosides. Elife *9*, e52611. https://doi.org/10.7554/eLife.52611.

48. Schueren, F., Lingner, T., George, R., Hofhuis, J., Dickel, C., Gärtner, J., and Thoms, S. (2014). Peroxisomal lactate dehydrogenase is generated by translational readthrough in mammals. Elife *3*, e03640. https://doi.org/10.7554/eLife.03640.

49. Lombardi, S., Testa, M.F., Pinotti, M., and Branchini, A. (2020). Molecular Insights into Determinants of Translational Readthrough and Implications for Nonsense Suppression Approaches. Int. J. Mol. Sci. *21*, 9449. https://doi.org/10.3390/ijms21249449.

50. Horibe, T., Torisawa, A., Akiyoshi, R., Hatta-Ohashi, Y., Suzuki, H., and Kawakami, K. (2014). Transfection efficiency of normal and cancer cell lines and monitoring of promoter activity by single-cell bioluminescence imaging. Luminescence *29*, 96–100. https://doi.org/10.1002/bio.2508.

51. Gilbreath, C., Ma, S., Yu, L., Sonavane, R., Roggero, C.M., Devineni, A., Mauck, R., Desai, N.B., Bagrodia, A., Kittler, R., et al. (2021). Dynamic differences between DNA damage repair responses in primary tumors and cell lines. Transl. Oncol. *14*, 100898. https://doi.org/10.1016/j.tranon.2020.100898.

52. Gu, S., Bodai, Z., Cowan, Q.T., and Komor, A.C. (2021). Base editors: Expanding the types of DNA damage products harnessed for genome editing. Gene Genome Ed. *1*, 100005. https://doi.org/10.1016/j.ggedit.2021.100005.

53. Nickoloff, J.A., Jones, D., Lee, S.-H., Williamson, E.A., and Hromas, R. (2017). Drugging the Cancers Addicted to DNA Repair. J. Natl. Cancer Inst. *109*, djx059. https://doi.org/10.1093/jnci/djx059.

54. Liu, S., Nyström, N.N., Kelly, J.J., Hamilton, A.M., Fu, Y., and Ronald, J.A. (2022). Molecular Imaging Reveals a High Degree of Cross-Seeding of Spontaneous Metastases in a Novel Mouse Model of Synchronous Bilateral Breast Cancer. Mol. Imaging Biol. *24*, 104–114. https://doi.org/10.1007/s11307-021-01630-z.

55. Hsu, P.D., Scott, D.A., Weinstein, J.A., Ran, F.A., Konermann, S., Agarwala, V., Li, Y., Fine, E.J., Wu, X., Shalem, O., et al. (2013). DNA targeting specificity of RNA-guided Cas9 nucleases. Nat. Biotechnol. *31*, 827–832. https://doi.org/10.1038/nbt.2647.

56. Shalaby, N., Kelly, J., Martinez, F., Fox, M., Qi, Q., Thiessen, J., Hicks, J., Scholl, T.J., and Ronald, J.A. (2022). A Human-derived Dual MRI/PET Reporter Gene System with High Translational Potential for Cell Tracking. Mol. Imaging Biol. *24*, 341–351. https://doi.org/10.1007/s11307-021-01697-8.

57. Dull, T., Zufferey, R., Kelly, M., Mandel, R.J., Nguyen, M., Trono, D., and Naldini, L. (1998). A third-generation lentivirus vector with a conditional packaging system. J. Virol. *72*, 8463–8471. https://doi.org/10.1128/JVI.72.11.8463-8471.1998.

58. Richter, M.F., Zhao, K.T., Eton, E., Lapinaite, A., Newby, G.A., Thuronyi, B.W., Wilson, C., Koblan, L.W., Zeng, J., Bauer, D.E., et al. (2020). Phage-assisted evolution of an adenine base editor with improved Cas domain compatibility and activity. Nat. Biotechnol. *38*, 883–891. https://doi.org/10.1038/s41587-020-0453-z.

59. Zafra, M.P., Schatoff, E.M., Katti, A., Foronda, M., Breinig, M., Schweitzer, A.Y., Simon, A., Han, T., Goswami, S., Montgomery, E., et al. (2018). Optimized base editors enable efficient editing in cells, organoids and mice. Nat. Biotechnol. *36*, 888–893. https://doi.org/10.1038/nbt.4194.

60. Kay, M.A., He, C.-Y., and Chen, Z.-Y. (2010). A robust system for production of minicircle DNA vectors. Nat. Biotechnol. *28*, 1287–1289. https://doi.org/10.1038/nbt.1708.

61. Xu, L., Liu, Y., and Han, R. (2019). BEAT: A Python Program to Quantify Base Editing from Sanger Sequencing. CRISPR J. *2*, 223–229. https://doi.org/10.1089/crispr.2019.0017.